

# Biosorption of Mercury (II) Ions, Congo Red Dye and Their Binary Mixture Using Chemically Activated Mango Leaves Powder

Mayowa Ezekiel Oladipo\*, Oluwaseun Adekoya Adelaja

Department of Chemistry, Federal University of Technology, Akure, Nigeria

## Abstract

The investigation of the potential of mango leaves powder activated with potassium persulphate ( $K_2S_2O_8$ ) solution for the removal of mercury (II) ions, Congo red (CR) dye and their binary mixture (BM) was carried out by characterizing the adsorbent (TMLP) using FTIR and conducting batch adsorption studies. The various adsorption parameters were optimized by comparing each adsorption's standard error of mean, in which the adsorption having the least SEM value with relative maximum removal efficiency was selected i.e. pH 7 (0.7325, 83.11%), contact time 30minutes (0.857, 63.82%), adsorbent dose 0.1g (1.5412, 50.46%), initial concentration 120mg/L (1.7388, 43%) and temperature 333K (0.248, 75%). The experimental equilibrium adsorption data of Hg (II) ions, CR dye and BM fitted best and well to Freundlich, Brunauer-Emmett-Teller and Langmuir respectively having 29.41, 21.28, 23.81mg/g as their respective maximum adsorption capacities. The kinetic data of all the adsorption conformed to the pseudo-second-order kinetic model due to low difference in  $q_{exp}$  and  $q_{cal}$  values, regression coefficient  $R^2 > 0.95$ , high initial sorption rate and lower values of validity models. The rate limiting step of each adsorption may be chemisorptions in this increasing order (binary mixture >  $Hg^{2+}$  > CR dye). The thermodynamic adsorption process of Hg (II) ions was spontaneous with the decrease in the degree of randomness and endothermic in nature, the adsorption of CR dye indicated non-spontaneous, increased randomness and endothermic process. At 323K, the adsorption of binary mixture became spontaneous with more random solid-solution interface and it was endothermic in nature.

## Keywords

Adsorption, Treated Mango Leaves Powder (TMLP), Mercury (II) Ions, Congo Red Dye, Binary Mixture

Received: July 13, 2019 / Accepted: September 20, 2019 / Published online: October 11, 2019

© 2019 The Authors. Published by American Institute of Science. This Open Access article is under the CC BY license.

<http://creativecommons.org/licenses/by/4.0/>

## 1. Introduction

The presence of heavy metals and dyes in the environment is a major worldwide concern due to their toxicity and carcinogenic effect on many life forms. Most of these wastes from industries such as mining, paint, paper and pulp, dye and textiles industries and many others, contain a lot of organic and inorganic particulates which could be biodegradable or non-biodegradable [1-2]. These particulates such as dyes (acid, basic, disperse, direct, mordant etc.); heavy metals like mercury, cadmium, copper, arsenic, lead

etc. accumulate at higher levels making water unpleasant to sight and gives a deteriorating effect.

Congo red (CR) is made from benzidine, which accumulates in living organism systems, the possibility of being metabolized through reductive cleavage of the azo group to give the aromatic amine derivative leads to serious health challenges such as: cancer, gastrointestinal irritation with nausea, vomiting, diarrhea, blurred vision, photophobia, chemical conjunctivitis, skin sensitization and corneal damage. Mercury enters into the environment as a pollutant from coal-fired power stations, residential coal burning for

\* Corresponding author

E-mail address: [oladipomayowa2222@gmail.com](mailto:oladipomayowa2222@gmail.com) (M. E. Oladipo)

heating and cooking, industrial process and waste incinerator. Once the mercury is in the environment, it is transformed by bacteria into methyl mercury ( $\text{CH}_3\text{Hg}$ ). The accumulation of this toxic mercury has reported in Japan between 1932 and 1968 which led to “minamata diseases” [3]. The effects on exposure to mercury are; genetic defects, neurological and behavioural disorders, tremors, insomnia, memory loss, neuromuscular effects, cognitive and motor dysfunction, chest pain, dyspnoea, headaches and kidney failure. Therefore, single and binary systems of CR and mercury (II) ions containing effluents have to be efficiently treated before they are discharged into water bodies or environment.

Physical, biological and chemical methods and technologies are commonly applied in removing dyes and heavy metals from aqueous solution. However, the application of some of these methods may be impractical due to economic constraints, insufficient to meet strict regulatory requirements and they may generate hazardous products which are difficult to treat [4]. Among of all these methods, adsorption is the most effective and non-destructive techniques that is widely used for the removal of dyes and heavy metals from aqueous solution due to its initial cost, simplicity of design, use of operation and insensitivity to toxic substances [5]. Adsorption is extensively used in industry for separation and purification of wastewater. Using of activated carbon as the adsorbent has been shown interested in due to its good capacity for adsorption of carcinogenic metals and dyes but its usage has been limited because of its high cost and about 10-15% loss during the regeneration [6]. Presently, researchers are interested in using biosorbents for removing dyes and heavy metals due to reusability of biomaterial, low operating cost, improved selectivity for specific metals/dyes of interest, removal of heavy metals/dyes from effluent irrespective of toxicity, short operation time, and no production of secondary compounds which might be toxic and possibility of metal/dye recovery and reuse.

Mango (*Mangifera indica*) is a fruit that belongs to the family Anacardiaceae. It is known around the world because of the dietary and essential vitamins such as Vitamins A, B, B<sub>6</sub>, C, E and K provided and its leaves are orange-pink when they are young and change rapidly to a dark gloss red. The leaves are dark green above and pale green below when matured. The main components are cellulose, hemicelluloses, pectins and lignin in which they provided different functional groups such as hydroxyl, carboxylic, amino and nitro groups which are important sites for adsorbate sorption [7].

The objective of this study was to investigate the potential of Treated Mango Leaves Powder (TMLP) as an alternative adsorbent for the removal of Congo red dye, Mercury (II) ions and their Binary mixture from aqueous solution. Characterization of TMLP was carried out using FTIR

analysis. The effect of pH, contact time, adsorbent dose, initial concentration, temperature was evaluated. Adsorption isotherms, kinetics and thermodynamic parameters were also evaluated and reported.

## 2. Materials and Methods

### 2.1. Adsorbent Collection, Preparation and Treatment

The unspotted mango leaves were plucked from the mango trees around FUTA campus.

This agricultural waste was thoroughly washed with running and distilled water to remove sand and other impurities; it was later submerged in the acid rinse (0.01M HCl) to remove soluble material. Then it was rinsed properly with distilled water and was sun-dry for 3days to dry up water from the leaves. Thereafter, it was oven-dried for 3hours at 105°C to ensure that it was free from moisture totally. It was grinded with the willey-mill; sieved with 250 $\mu\text{m}$  mesh sieve so as to have homogenized particle size.

The pulverized mango leaves powder was masticated with the solution of potassium persulphate ( $\text{K}_2\text{S}_2\text{O}_8$ ), it was allowed to stand for 2 hours at room temperature (30.8°C) measured using infrared thermometer, the mixture was rinsed with distilled water into the crucible and heated at 80°C inside the oven. It was re-grinded with mortar and pestle. Thereafter, it was stored in air-tight container labeled TMLP.

### 2.2. Preparation of Adsorbate Solution

Analytical grade of  $\text{HgCl}_2$  and CR dye were obtained from the laboratory.

A stock solution of mercury (II) ions of concentration 2000mg/L was prepared by dissolving 1g of mercuric chloride in 500mL distilled water. Its working standards were prepared by diluting the mercury (II) ions stock solution into final volume of 3mL of concentration (30, 60, 90, 120 and 150mg/L) with diphenylthiocarbazone ( $1.45 \times 10^{-3}\text{M}$ ) in a ratio of 1:2 with respective adding of 30 $\mu\text{L}$  of  $\text{H}_2\text{SO}_4$  (4.5M), 1500 $\mu\text{L}$  of 1,4-dioxane and 471 $\mu\text{L}$  of distilled water [8].

A stock solution of CR dye of concentration 2000mg/L was prepared by dissolving 1g of CR dye powder in 500mL distilled water. Its working standards were prepared by diluting CR dye stock solution into final volume of 3mL of concentration ranged from 30, 60, 90, 120 and 150mg/L.

### 2.3. Adsorbent Characterization

Fourier Transform Infra-Red (FTIR) Spectrophotometer (Shimadzu-8400S) was used to identify the different

functional groups available on the TMLP sites that aided the adsorption process. It was determined before adsorption and the FTIR spectrum was recorded within the wave number range 4000 – 500cm<sup>-1</sup>.

### 2.4. Batch Adsorption Experiments

The batch adsorption studies of Hg<sup>2+</sup>, CR dye and their binary mixture onto TMLP were conducted in a 250mL Erlenmeyer flask containing 0.1g of adsorbent with either 50mL of 60mg/L Hg (II) solution for mercury (II) ions determination, 50mL of 60mg/L Congo red dye solution for Congo red dye determination or addition of 50mL of 60mg/L Congo red dye solution and 50mL of 60mg/L Hg(II) solution to make binary mixture for Hg<sup>2+</sup> and Congo red dye determination. The mixtures in the flasks were agitated on an orbital shaker at constant speed of 100 rpm. The effect of pH (4, 5, 6, 7, 8 and 9), contact time (30, 60, 90, 120 and 150min), adsorbent dose (0.05, 0.1, 0.15, 0.2 and 0.25g), initial concentration (30, 60, 90 and 120mg/L) and temperature (303, 313, 323 and 333K) were evaluated. After agitation of 2 hours, each sample was filtered using Whatman filter paper no. 42 and the supernatant was refrigerated in the refrigerator (Midea HD-276F) until the final concentrations of Hg<sup>2+</sup> and CR dye were analyzed in the supernatant solutions using UV-visible Spectrophotometer (UNICAM UV HELIOS β) at a λ<sub>max</sub> of 488nm and 497nm respectively. The pH of the solution was adjusted with 0.1M HCl or NaOH.

Congo red sample was read colorimetrically without further adding of reagent because of the conjugated compounds presence but mercury (II) ions sample was read colorimetrically by pipetting 120μL of mercury (II) sample with respective adding of 240μL diphenylthiocarbazone (1.45×10<sup>-3</sup>M), 30μL of H<sub>2</sub>SO<sub>4</sub> (4.5M), 1500μL of 1,4-dioxane and 1110μL of distilled water.

The percentage adsorption of Hg<sup>2+</sup>/CR dye was determined using

$$\% \text{ Removal} = \frac{C_o - C_e}{C_o} \times 100$$

The amount of Hg<sup>2+</sup>/CR dye adsorbed (mg) per unit mass of adsorbent was obtained by using

$$q_e = \frac{(C_o - C_e)V}{m}$$

Where  $q_e$  is amount of metal ion adsorbed per gram of adsorbent (mgg<sup>-1</sup>),  $C_o$  is the initial metal ion concentration (mg L<sup>-1</sup>),  $C_e$  is the final metal ion concentration (mg L<sup>-1</sup>),  $V$  is the volume of the reaction mixture in liter, and  $m$  is the weight of adsorbent in the reaction mixture in g.

## 2.5. Adsorption Isotherm

In this present study, Langmuir, Freundlich and Brunauer-Emmett-Teller (BET) isotherm model were used to describe the sorption equilibrium.

### 2.5.1. Langmuir Isotherm

It predicts the existence of monolayer coverage of the adsorbate on the outer surface of adsorbent [9].

The linear form of Langmuir isotherm equation is given as

$$\frac{C_e}{q_e} = \frac{1}{q_m} K_L + \frac{C_e}{q_m}$$

Where  $C_e$  is the equilibrium concentration of adsorbate (mg/L),  $q_e$  is the amount of adsorbate adsorbed at equilibrium (mg/g),  $q_m$  is the monolayer adsorption capacity of the adsorbent (mg/g) and  $K_L$  is the Langmuir adsorption constant (L/mg).

### 2.5.2. Freundlich Isotherm

It assumes a heterogeneous surface (multi-layer) with a non-uniform distribution of heat of biosorption over the surface [10].

The linearized Freundlich model is represented by the equation:

$$\log q_e = \log K_F + \frac{1}{n} \log C_e$$

Where  $K_F$  and  $n$  are constant related to the sorption capacity and intensity.

### 2.5.3. Brunauer-Emmett-Teller (BET) Isotherm

It assumed that the adsorbate molecules could be adsorbed in more than one layer thickness on the surface of adsorbent [11]. The linearized Brunauer-Emmett-Teller model is represented by the equation:

$$\frac{C_e}{(C_s - C_e)q_e} = \frac{1}{K_b q_m} + \left( \frac{K_b - 1}{K_b q_m} \right) \left( \frac{C_e}{C_s} \right)$$

Where  $K_b$  and  $C_s$  are BET constant and solute concentration at the saturation of all layers (mg/L).

## 2.6. Adsorption Kinetics

Pseudo-first order kinetic and pseudo-second order kinetic model were used in this study to give insight into the reaction pathways, the mechanism of adsorption reactions and the solute uptake rate [12].

### 2.6.1. Pseudo-First Order Kinetic Model

The linear form of the pseudo-first order kinetic model is represented by

$$\ln(q_e - q_t) = \ln q_e - k_1 t$$

The values of  $k_1$  and calculated  $q_e$  can be determined from the slope and intercept respectively. Where  $q_e$  is the amount of solute adsorbed at equilibrium (mg/g),  $q_t$  is the amount of solute adsorbed at time  $t$  (mg/g),  $k_1$  pseudo first-order rate constant ( $\text{min}^{-1}$ ).

### 2.6.2. Pseudo-Second Order Kinetic Model

The linearized pseudo-second order kinetic model equation is represented by

$$\frac{t}{q_t} = \frac{1}{h} + \frac{1}{q_e} t$$

The values of calculated  $q_e$  and  $h$  can be determined from the slope and intercept respectively in the plot of  $t/q_t$  versus  $t$ .

Where  $k_2$  is pseudo second-order rate constant ( $\text{g/mg min}$ ) and the initial sorption rate,  $h$  ( $\text{mg.g}^{-1}.\text{min}^{-1}$ ) is expressed as:

$$h = k_2 q_e^2$$

### 2.7. Adsorption Thermodynamics

The thermodynamic parameters are the standard change in Gibbs free energy ( $\Delta G^\circ$ ), the standard change in entropy ( $\Delta S^\circ$ ) and the standard change in enthalpy ( $\Delta H^\circ$ ). It helps to understand the nature of the adsorption of adsorbate onto adsorbent [13]. These parameters are determined using the following equation:

$$-\Delta G^\circ = RT \ln K_o$$

Where  $T$  (K) is the solution temperature,  $R$  is the universal gas constant which is  $8.314 \text{ J/mol K}$  the distribution coefficient of the adsorbent,  $K_o$  is expressed:

$$K_o = \frac{q_e}{C_e}$$

### 2.8. Statistical Validity

The optimization of each effect of the factor that affected the adsorption was evaluated by the standard error of mean (SEM) equation shown below.

$$SEM = \frac{s}{\sqrt{N}}$$

Where  $n$  is the number of observation and the standard deviation,  $s$  is expressed as

$$s = \sqrt{\frac{\sum_{i=1}^n (q_{e,cal} - q_{e,exp})^2}{n-1}}$$

For the adsorption kinetics, the sum of square error (SSE) and Chi-square test ( $\chi^2$ ) are used.

$$SSE = \sum_{i=1}^n (q_{e,cal} - q_{e,exp})^2$$

$$\chi^2 = \sum_{i=1}^n \frac{(q_{e,exp} - q_{e,cal})}{q_{e,cal}}$$

The lower values of the validity models are strong clues of the applicability of adsorption kinetic model [14].

## 3. Results and Discussion

### 3.1. Adsorbent Characterization

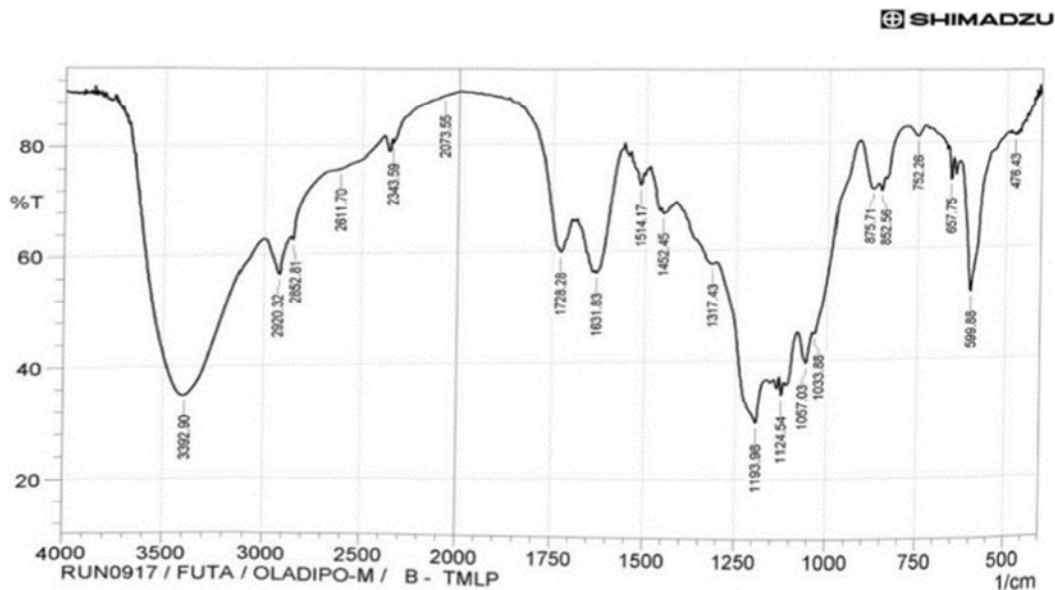


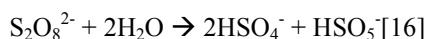
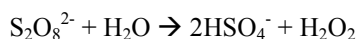
Figure 1. Fourier Transform Infra-Red Spectra of TMLP.

FTIR spectrum of TMLP at Figure 1 displayed various peaks at 3392.90cm<sup>-1</sup> (O-H stretching) 2920.32cm<sup>-1</sup> (C-H stretching of alcohol or carboxylic acid), 1631.83cm<sup>-1</sup> (C=C stretching), 1057.03cm<sup>-1</sup> (C-O stretching), 780.6cm<sup>-1</sup> (C-H stretching in aromatic ring), 599.88cm<sup>-1</sup> (asymmetric bending of SO<sub>4</sub> group), 476.43cm<sup>-1</sup> (symmetric bending of SO<sub>4</sub> group). These functional groups serve as the available binding sites for the adsorption to be aided by forming hydrogen bonding with the adsorbates [15].

### 3.2. Adsorption Parameters

#### 3.2.1. Effect of pH

The influence of pH on the adsorption of Hg<sup>2+</sup>, CR and their binary mixture onto TMLP is illustrated in Figure 2. It was observed that the percentage removal of Hg<sup>2+</sup>, CR and the binary mixture by TMLP decreased from (88.1% to 45.24%), (66.94% to 56.94%) and (70.34 to 69.43%) respectively as pH increased from 4 to 9. The following reactions occurred to the persulphate anion in the aqueous solution at lower and higher pH respectively.



The decrease in removal efficiency with increase in pH can be attributed to the fact that at low pH values, the hydrogen peroxide formed acts as an oxidizing agent that deprotonate the high concentration of H<sup>+</sup> species which allowed Hg<sup>2+</sup> to be adsorbed. While at high pH values, the anionic compounds tend to hinder the formation of Hg(Cl)OH and Hg(OH)<sub>2</sub> species which unable Hg<sup>2+</sup> to be adsorbed.

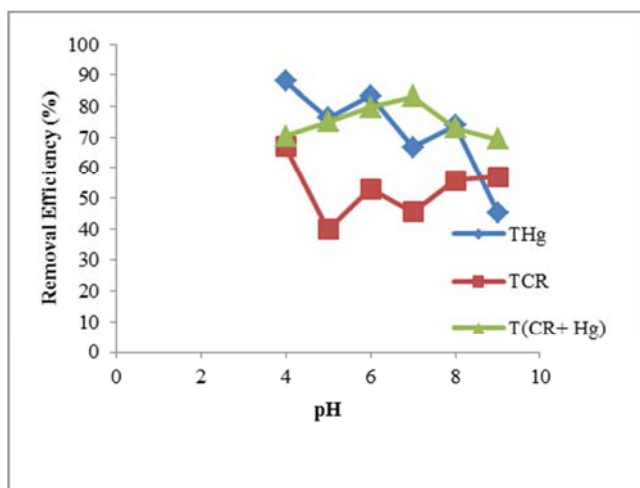


**Figure 2.** Effect of pH change on removal efficiency (%) of Hg<sup>2+</sup>, CR and the binary mixture. (Initial concentration=60mg/L, Agitation speed=100rpm, Contact time=2hours, Adsorbent dosage=0.1g). SEM of Hg<sup>2+</sup>=1.86, CR dye=1.16, BM=0.73.

The surface of the adsorbent become more protonated at low

pH values that make CR dye which is anionic dye to bind with the carbon at the surface of the adsorbent easily and at higher pH, hydroxyl ion increases which competes with the anionic dye for sorption site. From pH 8 and 9, there was increased in the removal efficiency which may be due to the fact that persulphate anion liberated two anionic compounds (HSO<sub>4</sub><sup>-</sup> and HSO<sub>5</sub><sup>-</sup>) that tend to reduce the competition between hydroxyl ion and CR dye which then makes the sorption site available for anionic dye.

Low adsorption of the binary mixture was attributed to the competition of the anionic groups between Congo red dye molecules and the amine groups on the adsorbents while its highadsorption was due the ability of Hg (II) ions to form covalent bonds with the anionic group on the adsorbents [17].

By comparing the standard error mean (SEM) of each adsorption, it was observed that the binary mixture adsorption had the least SEM value (0.73) in whose the relative maximum removal efficiency (83.11%) at pH 7 was selected. Therefore, in the subsequent work, experiments were carried out at fixed optimum of pH 7.

#### 3.2.2. Effect of Contact Time

The effect of contact time on removal of Hg<sup>2+</sup>, CR and their binary mixture is portrayed in Figure 3.

It was observed that there was a fast sorption of Hg (II) ions on the surface of TMLP for the first 30 minutes (59.524%) which was due to the availability of active sites at the surface of the adsorbent for quick binding with Hg (II) ions [18]. It decreases gradually as at 60minutes (50%), which was as a result of the positive interfering ions that competed with Hg (II) ions for binding on the adsorbent's surface. It achieved its equilibrium contact time at 90minutes (64.286%) as a result of the binding sites that became exhausted. Later, the percentage removal decreased at 120minutes and later increased at 150minutes due to the contribution of persulphate anions to the physicochemical interactions between the biomass and the metal solution [19].

At the initial stage, the sorption rate was rapid at first 30 minutes (33.89%) which was as a result of the active sites on the adsorbent's surface that were ready to bind with CR dye in the wastewater. At the later stage, there was diffusion of the dyes into the inner part of the adsorbent which led to slower adsorption rate [20]. The equilibrium is achieved at 120 minutes (81.25%) as a result of the binding sites that became exhausted. The percentage removal gradually slowed down to 70.56% due to the repulsive forces between the molecules on the adsorbent and the bulk phase [21-22]. Similar trend has been reported by the adsorption of CR dye from aqueous solution onto Bread fruit seed shell powder [23].

The adsorption of the binary mixture reached its equilibrium at 30 minutes which was due to the fact that initially all the adsorbent sites are vacant and solute concentration is very high [24]. The removal efficiency decreases gradually as a result of less availability of the active sites.

The standard error mean (SEM) of each adsorption was compared for contact time, it was found that the binary mixture adsorption had the least SEM value (0.86) in whose the relative maximum removal efficiency (63.82%). Therefore, in the subsequent work, experiments were carried out at fixed optimum of 30 minutes.

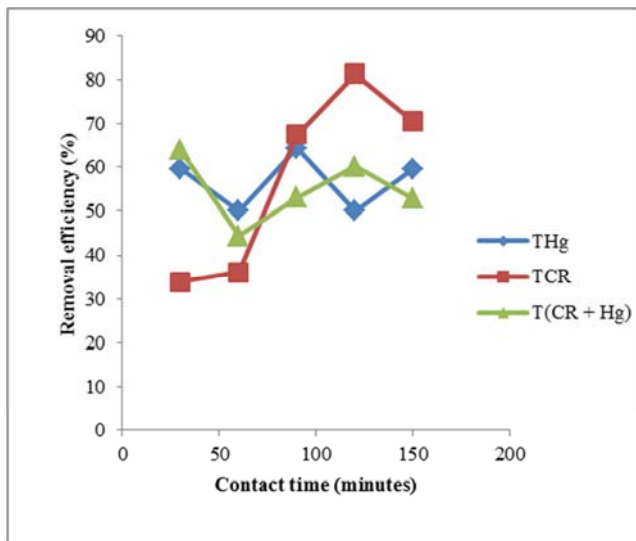


**Figure 3.** Effect of contact time on removal efficiency (%) of  $Hg^{2+}$ , CR and the binary mixture (pH=7.0, Initial concentration=60mg/L, Agitation speed=100rpm, Adsorbent dosage=0.1g). SEM of  $Hg^{2+}$ =2.0415, CR dye=2.8844, BM=0.8571.

### 3.2.3. Effect of Adsorbent Dose

It is evident from Figure 4 that shows the effect of adsorbent dose on the removal of  $Hg^{2+}$ , CR and their binary mixture that the  $Hg^{2+}$  removal reached its equilibrium twice at adsorbent doses 0.05g and 0.2g. It was due to the greater availability of specific surfaces of the adsorbent at these two points. However, there were slight changes in removal efficiency beyond 0.05g and 0.2g which can also be as a result of the overlapping of the negatively charged ions at the surface of the adsorbents [25].

The percentage removal of CR dye increased with increase in the adsorbent dose. This was as a result of increase in the number of active sites on TMLP with the increase in the adsorbent dosages [26]. At 0.2g, there was a slight drop in removal efficiency due to the aggregation of the binding sites.

By comparing the adsorption trend of each solute, it was observed that at lower adsorbent dosage, there was more overlapping of the positively charged ions than the negatively charged ions and at higher adsorbent dosage, it was vice-

versa. The adsorption of binary mixture onto TMLP, it can be deduced that persulphate anions released into the aqueous solution  $HSO_4^-$  &  $HSO_5^-$  anions contributed greatly to the reduction of the overlapping strength of positively charged ions at lower adsorbent dose. At higher adsorbent dose, potassium ion  $K^+$  reduced the overlapping force of the negatively charged ions. There was partial aggregation that occurs at adsorbent dose 0.15g, which resulted in decreasing the number of active sites on the surface of biomass [27-28].

The standard error mean (SEM) of each adsorption was compared for adsorbent dosage, it was found that the adsorption of the binary mixture had the least SEM value (1.547) in whose the relative maximum removal efficiency (50.46%) at adsorbent dose of 0.1g. Therefore, in the subsequent work, experiments were carried out at fixed optimum of 0.1g.

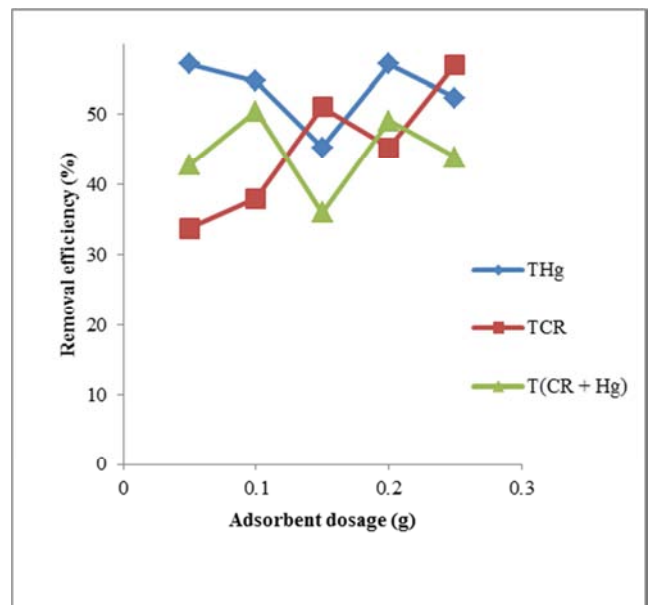


**Figure 4.** Effect of adsorbent dosage on removal efficiency (%) of  $Hg^{2+}$ , CR and the binary mixture (pH=7.0, Initial concentration=60mg/L, Agitation speed=100rpm, Contact time=30 minutes). SEM of  $Hg^{2+}$ =5.1315, CR dye=2.4616, BM=1.5472.

### 3.2.4. Effect of Initial Concentration

The effect of initial concentration on removal of  $Hg^{2+}$ , CR and their binary mixture is illustrated in Figure 5. At low concentration, adsorption rate increased due to the concentration gradient that contributed as the driving force of the adsorbate into the TMLP. As the concentration is high, the  $Hg^{2+}$  removal rate decreased which was caused by the saturation of some active adsorption sites. The result is in agreement to M. A. Ashraf *et al.*, [29].

It can be deduced that at low concentrations there will be availability of the active sites on the TMLP surface. From CR dye concentration of 60mg/L, the active sites required for the adsorption of dye lack which eventually retards the overall

adsorption. Similar work by Deepak Pathania *et al* [24] supported this assertion. At the concentration of 90mg/L to 120mg/L, the concentration gradient contributed to the removal efficiency of CR dye which allowed it to experience equilibrium at 120mg/L.

The removal efficiency of binary mixture onto TMLP decreased as the initial concentration increased from 30mg/L to 120mg/L (57.13% - 29.76%) which was as a result of the mass transfer of the binary mixture between the solvent and solute phase that overcome the concentration gradient of the adsorption process.

The standard error mean (SEM) of each adsorption was compared for initial concentration, it was found that the adsorption of Congo red dye had the least SEM value (1.739) in whose the relative maximum removal efficiency (43%) at initial concentration of 120mg/L. Therefore, in the subsequent work, experiments were carried out at fixed optimum of 120mg/L.

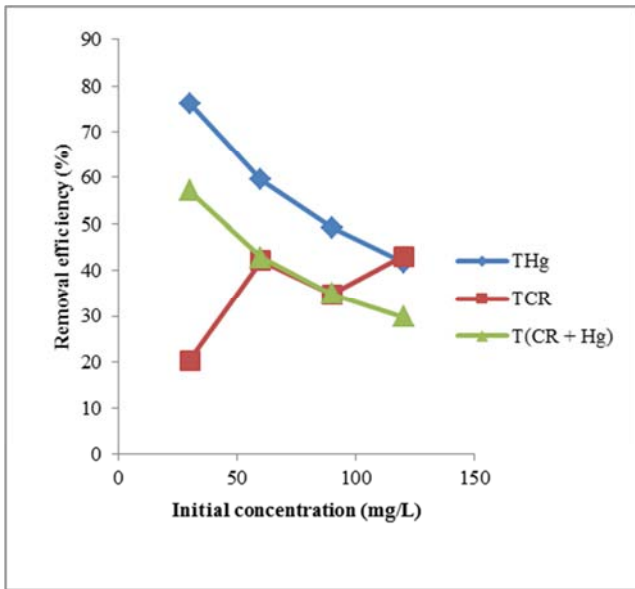


**Figure 5.** Effect of initial concentration on removal efficiency (%) of Hg<sup>2+</sup>, CR and the binary mixture. (pH=7.0, Initial concentration=60mg/L, Agitation speed=100rpm, Contact time=30 minutes, Adsorbent dosage=0.1g). SEM of Hg<sup>2+</sup>=2.9513, CR dye=1.7388, BM=2.006426.

### 3.2.5. Effect of Temperature

The influence of temperature on the percentage removal of Hg<sup>2+</sup>, CR dye and the binary mixture by TMLP is shown in Figure 6.

At the initial stage, increase in temperature increased the Hg<sup>2+</sup> uptake capacity which was due to an enhanced rate of intra-particle diffusion of Hg<sup>2+</sup> into the pores of the adsorbent [30-31]. Optimum removal capacity of Hg<sup>2+</sup> was obtained at 313K; similar result was supported by Muhammad H. R *et al.*, [32]. Beyond 313K, the increase in temperature leads to decrease in Hg<sup>2+</sup> uptake which was due to the increase in the

retarding forces acting on the diffusing ions. At the final stage of the temperature range, the percentage removal increased as a result of the interaction of the solute and adsorbent.

It was observed that as temperature increases, the percentage removal of CR dye increased which was attributed to an increase in the mobility of the large dye ions and penetration into the TMLP surface as the result of the enlargement of pore size of the adsorbents [33-34]. Beyond 313K, the solute was more difficult to adsorb which led to steady sorption.

For the adsorption of binary mixture onto TMLP, it was observed that as the temperature increased the removal efficiency of the binary mixture increased which was due to the increase in the mobility of both dye and Hg (II) ions in the binary solution which were penetrated into the TMLP surface. At a temperature of 323K, it has its optimal removal efficiency (67.23%). As the temperature increases from 323K, the removal efficiency decreased to 61.25% which can be attributed to CR dye solubility i.e. the interaction between the solute and the solvent is stronger than that between the solute and the adsorbent [23].

By comparing the standard error mean (SEM) of each adsorption, it was observed that the adsorption of Hg<sup>2+</sup> had the least SEM value (0.248) in whose the relative maximum removal efficiency (75%) at temperature 333K was selected.

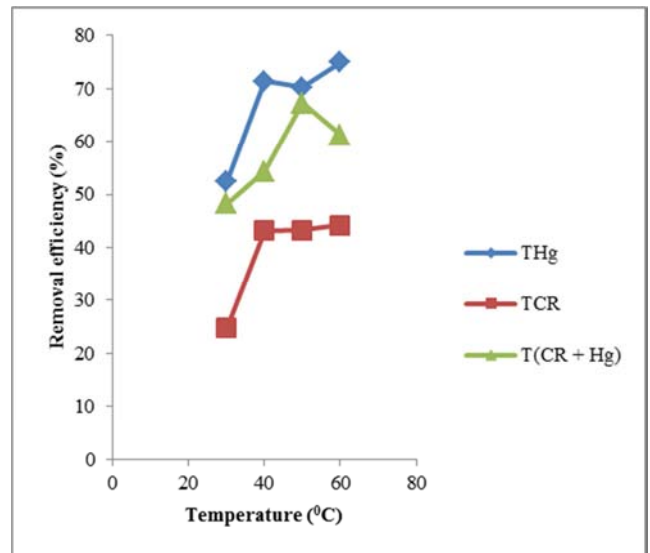


**Figure 6.** Effect of temperature on removal efficiency (%) of Hg<sup>2+</sup>, CR and the binary mixture. (pH=7.0, Initial concentration=120mg/L, Agitation speed=100rpm, Contact time=30 minutes, Adsorbent dosage=0.1g). SEM of Hg<sup>2+</sup>=0.248, CR dye=2.947429, BM=2.826041.

### 3.3. Adsorption Isotherm

Figures 7, 8 and 9 depicted the Langmuir, Freundlich and Brunauer-Emmett-Teller (BET) models plot of the adsorption of Hg<sup>2+</sup>, CR dye and their binary mixture onto TMLP. The isotherm parameters and values of correlation coefficient are

shown in Table 1.

It is evident from the plots and the values of correlation coefficient  $R^2$  (Table 1) that the Langmuir isotherms model is efficient in describing the adsorption of binary mixture onto TMLP, Freundlich isotherm model is efficient in describing the adsorption of a single solute system i.e. adsorption of  $Hg^{2+}$  onto TMLP. Finally, BET model is efficient in describing the adsorption of Congo red dye onto TMLP because the adsorbate molecules adsorbed in more than one layer thickness on the surface of adsorbent.

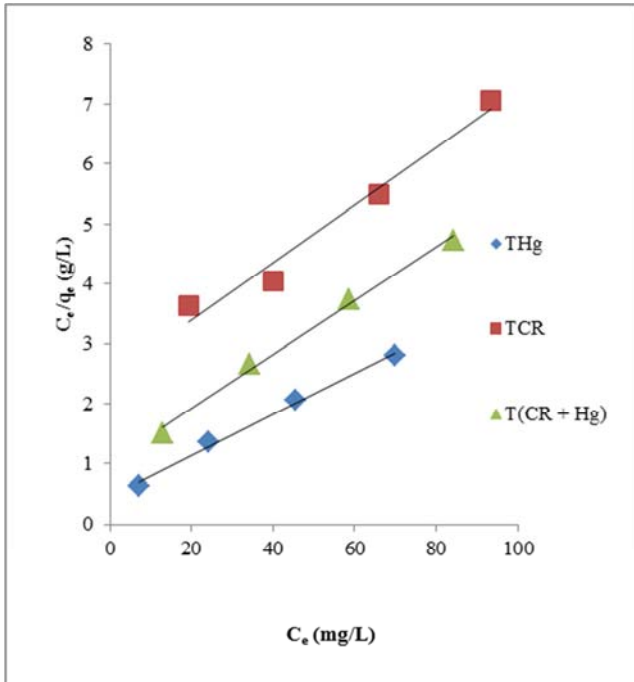


Figure 7. Langmuir isotherm plot for the sorption of mercury (II) ions, Congo red dye and the binary mixture by TMLP.

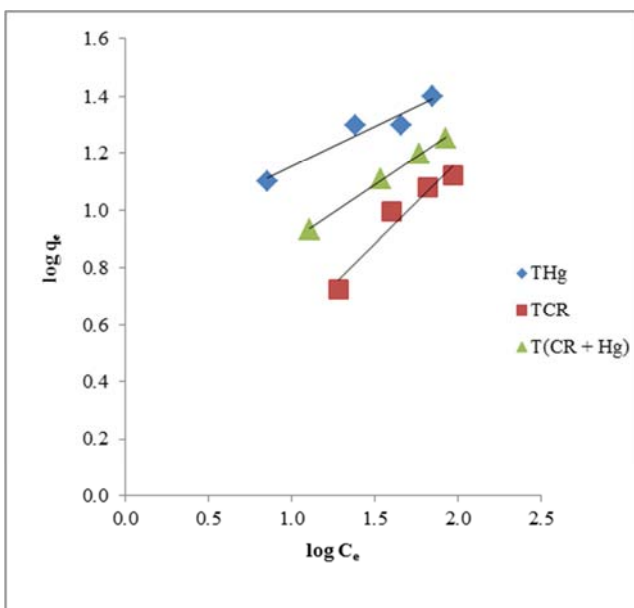


Figure 8. Freundlich isotherm plot for the sorption of mercury (II) ions, Congo red dye and the binary mixture by TMLP.

Table 1. The isotherm parameters and values of correlation coefficient for the adsorption of Mercury (II) ions, CR dye and their binary mixture onto TMLP.

ISOTHERM PARAMETERS	Hg (II) ions	Congo red dye	Binary mixture
Langmuir			
$q_m$ (mg/g)	29.41	21.28	23.81
$K_L$ (L/mg)	0.075	0.019	0.07
$R^2$	0.994	0.9732	0.9989
$R_L$	0.1509	0.4124	0.16
Freundlich			
$n$	2.89	1.724	2.976
$K_F$ (mg/g)	5.34	1.026	4.764
$R^2$	0.9982	0.9458	0.9881
Brunauer-Emmett-Teller			
$q_m$ (mg/g)	0.0096	0.015	0.047
$K_B$	-0.66	-3.45	-2.287
$R^2$	0.9359	0.9871	0.9448

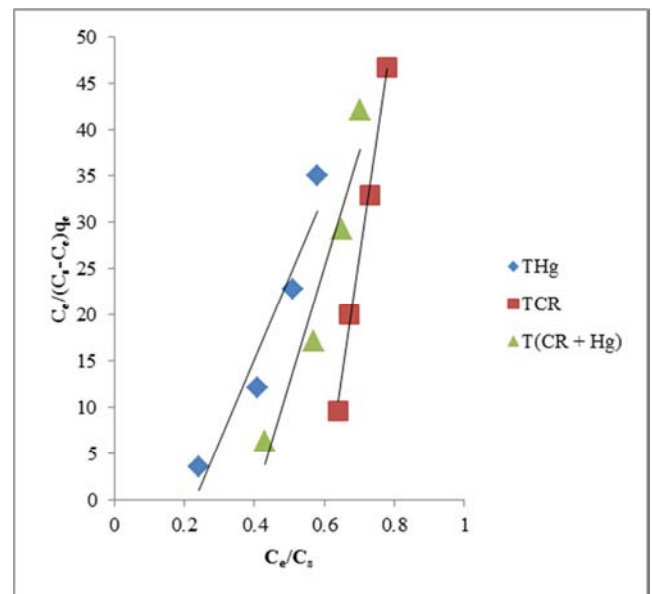


Figure 9. Brunauer-Emmett-Teller isotherm plot for the sorption of mercury (II) ions, Congo red dye and their binary by TMLP.

### 3.4. Adsorption Kinetics

Pseudo-first order and pseudo-second order kinetic models were applied in this study to investigate the reaction pathways and potential rate limiting steps of the adsorption of  $Hg^{2+}$ , CR dye and the binary mixture onto TMLP. The pseudo-first-order and pseudo-second-order plots are shown in Figures 10 and 11 respectively with their parameters given in Table 2.

From kinetic model parameters presented in Table 2, pseudo-first order model results showed high difference in  $q_{exp}$  and  $q_{cal}$  values coupled with regression coefficient,  $R^2 < 0.95$  and larger values of SSE and  $\chi^2$ . It suggested that the kinetic data was inadequacy for the pseudo-first-order model. The line graph of the adsorption of  $Hg^{2+}$  followed pseudo-second order plot which the rate constant ( $k_1$ ) to have negative value.

From the angle of pseudo-second-order model, it can be



deduced that there is low difference in  $q_{exp}$  and  $q_{cal}$  values, regression coefficient  $R^2 > 0.95$ , high initial sorption rate and lower values of validity models indicated that the kinetic data was fitted for the pseudo-second-order model. Due to the high values of the initial sorption rate  $h$ , it can be said that the rate control of the adsorption process by chemisorptions increased from the adsorption of binary mixture  $> Hg^{2+} > CR$  dye onto TMLP.

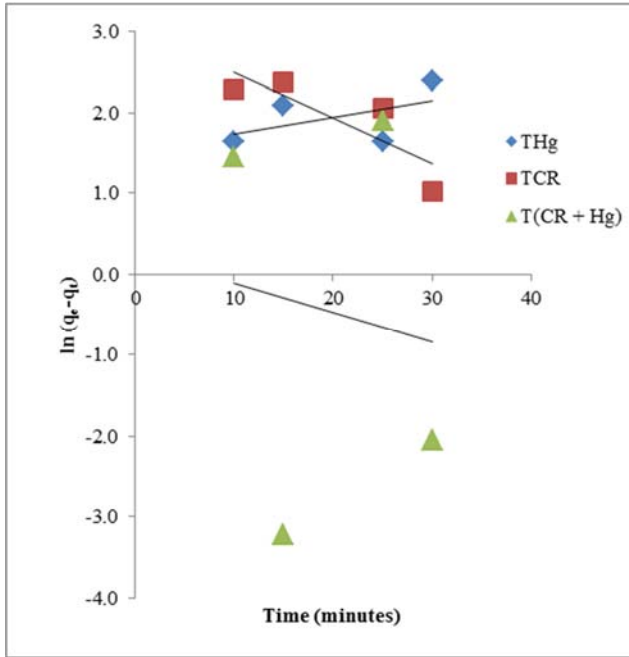


Figure 10. Pseudo-first order plot for adsorption of  $Hg^{2+}$ , CR dye and binary mixture onto TMLP.

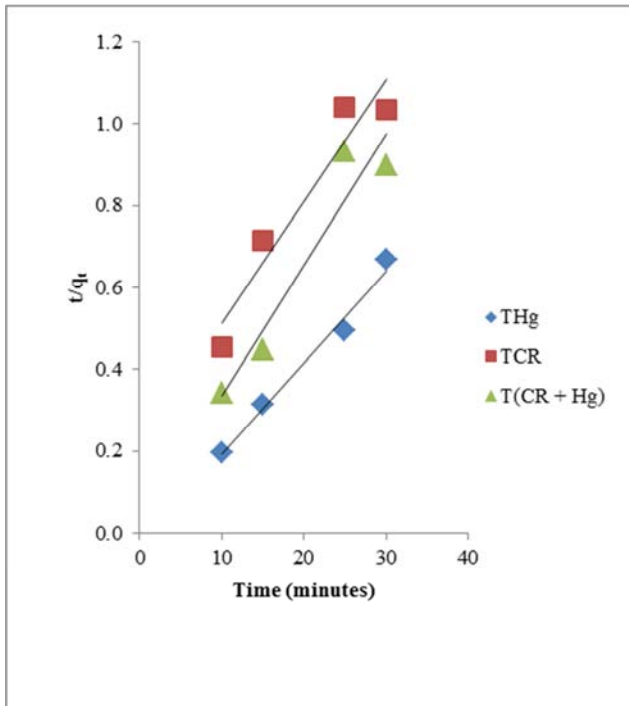


Figure 11. Pseudo-second order plot for adsorption of  $Hg^{2+}$ , CR dye and binary mixture onto TMLP.

Table 2. Kinetic model parameters with the statistical validity models of the adsorption of  $Hg^{2+}$ , CR dye and binary mixture onto TMLP.

KINETIC PARAMETERS	Hg (II) ions	Congo red dye	Binary mixture
$q_{exp}$ (mg/g)	51.9	31.79	33.55
Pseudo-first order			
$q_{cal}$ (mg/g)	4.586	21.52	1.297
$k_1$ ( $min^{-1}$ )	-0.02	0.056	0.036
$R^2$	0.277	0.695	0.017
SSE	559.6536	26.3682	260.064
$\chi^2$	23.657	5.135	16.1265
Pseudo-second order			
$q_{cal}$ (mg/g)	45.46	34.48	31.25
$k_2$ (g/mg min)	0.0167	0.00389	0.0683
$h$ (mg/g min)	34.48	34.630	66.67
$R^2$	0.983	0.923	0.92
SSE	10.3684	1.809	1.3225
$\chi^2$	3.22	1.345	1.15

### 3.5. Adsorption Thermodynamics

Van't Hoff plot for the adsorption of  $Hg^{2+}$ , CR dye and binary mixture onto TMLP is shown in Figure 12. Table 3 presents the values of the thermodynamic quantities ( $\Delta S^0$ ,  $\Delta H^0$  and  $\Delta G^0$ ) obtained from the plot and equation.

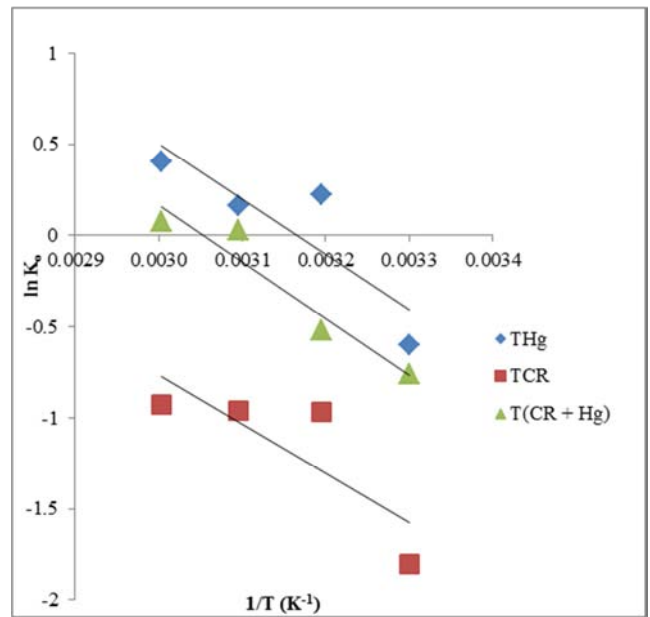


Figure 12. Van't Hoff plot for the adsorption of  $Hg^{2+}$ , CR dye, and binary mixture onto TMLP.

Positive  $\Delta H^0$  values for the adsorption of  $Hg^{2+}$ , CR and binary mixture indicated the endothermic nature of adsorption process. Similar positive values have been reported by other researchers [35].

The positive  $\Delta S^0$  values for the adsorption of CR dye and binary mixture showed the existence of the molecules in solution is less random than that on surface [36] while the negative  $\Delta S^0$  values of the adsorption of  $Hg^{2+}$  indicated that no significant change occurred in the internal structure of the active site of the adsorbents.

The negative  $\Delta G^0$  values of the adsorption of  $Hg^{2+}$  from 313-333K indicated the viability, feasibility, and spontaneity of the adsorption process while the positive  $\Delta G^0$  values of the adsorption of CR and binary mixture showed non-

spontaneity of the adsorption process. At temperature of 323K, the  $\Delta G^0$  value of the binary mixture was negative and made the adsorption process to be spontaneous at this point.

**Table 3.** Thermodynamic parameters for the adsorption of mercury (II) ions, Congo red dye and the binary mixture onto TMLP at different temperatures.

Thermodynamic parameters	TEMPERATURE (K)			
	303K	313K	323K	333K
Mercury(II) ions				
$\Delta G$ (KJ/mol)	1.506	-0.58	-0.45	-1.12
$\Delta H$ (KJ/mol)				25.06
$\Delta S$ (J/mol. K)				79.32
Congo red dye				
$\Delta G$ (KJ/mol)	4.55	2.52	2.59	-0.07
$\Delta H$ (KJ/mol)				21.87
$\Delta S$ (J/mol. K)				59.10
Binary mixture				
$\Delta G$ (KJ/mol)	1.92	1.35	-0.07	0.21
$\Delta H$ (KJ/mol)			25.71	
$\Delta S$ (J/mol. K)			78.50	

## 4. Conclusion

The present study revealed the potential of treated mango leaves powder (TMLP) for the removal of Hg (II) ions, CR dye and their binary mixture from aqueous solution. The optimum conditions for all the batch adsorption studies were found to be pH (7.0), contact time (30mins), adsorbent dose (0.1g), initial concentration (120mg/L) and temperature (333K). The study on equilibrium data showed that Freundlich, Langmuir and BET isotherm model fitted well to the adsorption of Hg (II) ions, CR dye and their binary mixture respectively. The kinetic studies revealed that all the adsorption processes followed the pseudo-second-order kinetic model.

The thermodynamic studies of the adsorption of  $Hg^{2+}$  and the adsorption of binary mixture at 323K were spontaneous. In this study, it can be concluded that the TMLP has the affinity and capacity to remove the investigated pollutants in this increased order (Mercury (II) ions>Binary mixture>Congo red dye).

## Conflict of Interest

The Authors declare that there are no conflicts of interest.

## References

- [1] Kadirvelu, K., Thamaraiselvi, K., & Namasivayam, C. (2001). Removal of heavy metal from industrial wastewaters by adsorption onto activated carbon prepared from an agricultural solid waste. *Bioresour. Technol.*, 76, 63-65.
- [2] Williams, C. J., Aderhold, D., & Eadyean, G. J. (1998). Comparison between biosorbents for the removal of metal ions from aqueous solutions. *Water Res.* 32, 216-224.
- [3] WHO Environmental Health Criteria 101, Methyl Mercury, Geneva, World Health Organization (1990) 68.
- [4] Reddad, Z., Gerente C., Andres, I., & Le Cloirec, P. (2002). Adsorption of several Metal Ions onto a Low-Cost Biosorbent: Kinetic and Equilibrium Studies. *Environmental Science & Technology*, 36, 2067-2073.
- [5] Uddin, M. T., Rukanuzzaman, M., Khan, M. M. R., & Islam, M. A. (2009). Adsorption of methylene blue from aqueous solution by jackfruit (*Artocarpusheteropyllus*) leaf powder: A fixed-bed column study. *Journal of Environment Management*, 90, 3443-3450.
- [6] Bhattacharyya, K. G., & Sharma, A. (2003). Adsorption Characteristic of the dye, Brilliant Green, on Neem leaf powder. *Dyes and Pigments*, 57, 211-222.
- [7] Ong, P. S., Ong, S. T., & Hung, Y. T. (2013). Utilization of mango leaf as a low-cost adsorbent for the removal of Cu(II) ions from aqueous solution. *Asian Journal of Chemistry*, 25 (11), 6141-6145.
- [8] Ahmed, M. J., & Alam, M. S. (2003). A rapid spectrophotometric method for the determination of mercury in environmental, biological, soil and plant samples using diphenylthiocarbazon. *Spectroscopy* 17, 45-52.
- [9] Langmuir, I. (1916). The constitutional and fundamental properties of solids and liquids, *J. Am. Chem. Soc.* 38, pp. 2221-2295.
- [10] Freundlich, H. M. F. (1906). Over the adsorption in solution, *Z. Phys. Chem.* 57, pp. 385-470.
- [11] Brunauer, S., Emmett, P. H., & Teller E. (1938). Adsorption of gases in multi molecular layers. *Journal of the American Chemical Society*, 60 (2), 309-319.
- [12] Ho, Y. S., & McKay, G. (1998). Kinetic model for Pb(II) sorption onto peat. *Adsorpt. Sci., Technol.*, 16, 943-955.
- [13] Birtukan, A., Khalid, S., & Nathan, M. (2015). Kinetic, equilibrium and thermodynamic study of 2-Chlorophenol adsorption onto *Ricinus Communis* pericarp activated carbon from aqueous solutions. *Green chemistry Letters and Reviews*, 8, 1-12. DOI: 10.1080/17518253.2015.1065348.

- [14] Adewumi O. D., Folahan A. A., & Ezekiel O. O. (2017). Kinetics, mechanism, isotherm and thermodynamic studies of liquid-phase adsorption of Pb<sup>2+</sup> onto wood activated carbon supported zerovalent iron (WAC-ZVI) nanocomposite. *Cogent Chemistry*, 3, 1351653.
- [15] Khan, T. A., Sharma, S., & Ali, I. (2011). Adsorption of Rhodamine B dye from aqueous solution onto acid activated mango (*Mangifera indica*) leaf powder: Equilibrium, kinetic and thermodynamic studies. *Journal of Toxicology and Environmental Health Sciences* Vol. 3 (10), pp. 286-297.
- [16] [http://www.peroxychem.com/media/90826/AOD\\_Brochure\\_Persulfate.pdf&ved=2ahUKewjC0uWrlJrdAhVCAsAKHa1bAg4QFjABegQICBAB&usq=AOvVaw38bEPGaMNHsd00nN9LanBt](http://www.peroxychem.com/media/90826/AOD_Brochure_Persulfate.pdf&ved=2ahUKewjC0uWrlJrdAhVCAsAKHa1bAg4QFjABegQICBAB&usq=AOvVaw38bEPGaMNHsd00nN9LanBt).
- [17] Yang, H., & Feng, Q. (2010). Characterization of pore-expanded amino-functionalized mesoporous silicas directly synthesized with dimethyldecylamine and its application for decolorization of sulfonated dyes. *J Hazard Mater* 180, 106-114.
- [18] Gupta, S., Kumar, D., & Gaur, J. P. (2008). Kinetics and isotherm modeling of lead (II) sorption onto some waste plant materials. *Chem. Eng. J.* 148 (2-3), 226-233.
- [19] Aslam, M., Rais, S., Alam, M., & Pugazhenzi, A. (2013). Adsorption of Hg (II) from Aqueous Solution Using *Adulsa* (*Justicia adhatoda*) Leaves Powder: Kinetic and Equilibrium Studies. *Journal of Chemistry*, Volume 2013, Article ID 174807, 11 pages. <http://dx.doi.org/10.1155/2013/174807>.
- [20] Umpuch, C., & Jutarat, B. (2013). Adsorption of organic dyes from aqueous solution by surfactant modified corn straw. *Inter. J. Chem. Eng. Applications*, 4 (3), 134-139.
- [21] Wu, C. H. (2007). Adsorption of reactive dyes onto carbon nanotubes: Equilibrium, kinetics and thermodynamics. *J. Hazard. Mater.* 144, 96-98.
- [22] Iscen, C. F., Krian, I., & Iihan, S. (2007). Biosorption of reactive black dyes by *Fenicillium restrictum*: the kinetic study. *J. Hazard Mater.* 143, 335-338.
- [23] Enenebeaku, K. C., Okorochoa, J. N., Enenebeaku, E. U., Anukan, B., Onyeocha, O. V., Ogukwe, E. C., & Oguzie, E. E. (2016). Adsorption of Congo Red Dye from Aqueous solution using Agricultural Waste. *IOSR Journal of Applied Chemistry (IOSR-JAC)*, Volume 9, 39-51.
- [24] Deepak, P., & Pardeep S. (2017). Removal of methylene blue by adsorption onto activated carbon developed from *Ficus Caricabast*. *Arabian journal of chemistry*, 10, 51445-51451.
- [25] Gebremedhin G. (2016). Removal of Chromium (VI) Ions from Aqueous Solution Using Leaves of *Cordia Africana* and Sawdust of *Acacia Albida*. *International Journal of Modern Chemistry and Applied Science*, 3 (2), 369-377.
- [26] Hassanein, T. F., & Koumanova, B. (2010). Evaluation of adsorption potential of the agricultural waste wheat straw on basic yellowish 21. *Journal of the University Chemical Technology and Metallurgy*, 45 (4), 407-414.
- [27] Gupta, S. S., & Bhattacharyya, K. G. (2008). Immobilization of Pb(II), Cd(II) and Ni(II) ions on kaolinite and montmorillonite surfaces from aqueous medium. *Journal of Environmental Management* 87, 46-58.
- [28] Viera, M. G. A., Neto, A. F. A., & Gimenes, M. I. (2010). Sorption kinetics and equilibrium for the removal of nickel ions from aqueous phase on calcined Bofebentonite clay. *Journal Hazardous Materials* 177, 362-371.
- [29] Muhammad, A. A., Maah, M. J., & Yusoff, I. (2010). Study of mango biomass (*Mangifera indica* L) as a cationic biosorbent. *International Journal of Environment Science & Technology* 7 (3), 581-590.
- [30] Bouhamed, F., Elouear, Z., & Bouzid, J. (2012). Adsorptive removal of copper (II) from aqueous solutions on activated carbon prepared from Tunisian date stones: Equilibrium, kinetics and thermodynamics. *Journal of the Taiwan Institute of Chemical Engineers* 43, 741-749.
- [31] Kalavathy, M. H., & Miranda, L. R. (2012). Comparison of copper adsorption from aqueous solution using modified and unmodified Heveabrsiliensis saw dust. *Desalination* 255, 1-7.
- [32] Muhammad, H. R., Aqsa, S., Umar, F., Makshoof, A., Tajamal, H., Adnan, M., & Muhammad, S. (2015). *Phragmites Karka* as a Biosorbent for the Removal of Mercury Metal ions from aqueous solution: Effect of Modification. *Hindawi Publishing Corporation Journal of Chemistry* Volume 2015, Article ID 293054, 12 pages.
- [33] Yu, L., & Ya-juan, L. (2008). Biosorption isotherms, kinetics and thermodynamics. *Separation and Purification Technology* 61 (3), 229-242.
- [34] Ayla, Ö., Gökem, G., Ayla, Ç., & Bahadır, K. K. (2009). Biosorption of copper (II) ions on *Enteromorpha prolifera*: application of response surface methodology (RSM). *Chemical Engineering Journal* 146 (3), 377-387.
- [35] Sathya, M., Kumarand, P. E., & Santhi M. (2017). Equilibrium Studies and Kinetics Mechanism for the Removal of Congo red by *Passiflora Foetida* Activated Carbon-MnO<sub>2</sub>- Nano Composite. *IOSR Journal of Applied Chemistry*, 10 (01), 8-14.
- [36] Yu, Y., Zhuang, Y. Y., Wang, Z. H., & Qiu, M. Q. (2004). *Chemosphere*, 54, 425-430.